PHYSICAL REVIEW D **86,** 094016 (2012)

Semi-inclusive photon-hadron production in pp and pA collisions at RHIC and LHC

Amir H. Rezaeian

Departamento de Física, Universidad Técnica Federico Santa María, Avenida España 1680, Casilla 110-V, Valparaiso, Chile

(Received 5 September 2012; published 6 November 2012)

We investigate semi-inclusive photon-hadron production in the color-glass-condensate framework at RHIC and the LHC energies in proton-proton (pp) and proton-nucleus (pA) collisions. We calculate the coincidence probability for azimuthal correlation of pairs of photon-hadron production and show that the away-side correlations have a double-peak or a single-peak structure depending on trigger particle selection and kinematics. This novel feature is unique for semi-inclusive photon-hadron production compared to a similar measurement for double inclusive dihadron production in pA collisions. We obtain necessary conditions between kinematic variables for the appearance of a double-peak or a single-peak structure for the away-side photon-hadron correlations in pp and pA collisions at forward rapidities and show that this feature is mainly controlled by the ratio $z_T = p_T^{\rm hadron}/p_T^{\rm photon}$. Decorrelation of away-side photon-hadron production by increasing the energy, rapidity and density, and appearance of double-peak structure can be understood by QCD saturation physics. We also provide predictions for the ratio of single inclusive prompt photon to hadron production, and the two-dimensional nuclear modification factor for the semi-inclusive photon-hadron pair production at RHIC and the LHC at forward rapidities.

DOI: 10.1103/PhysRevD.86.094016 PACS numbers: 25.75.Bh, 13.60.Hb, 13.40.−f, 25.75.Cj

I. INTRODUCTION

It is generally believed that a system of partons (gluons) at high-energy (or small Bjorken-x) forms a new state of matter where the gluon distribution saturates [1]. Such a system is endowed with a new dynamical momentum scale, the so-called saturation scale at which nonlinear gluon recombination effects become as important as the gluon radiation. The color-glass-condensate (CGC) approach has been proposed to study the physics of gluon saturation at the small-x region [2,3]. The CGC formalism is an effective perturbative quantum chromodynamics (pQCD) theory in which one systematically resums quantum corrections, which are enhanced by large logarithms of $1/x$ and also incorporates nonlinear high gluon density effects. In the CGC approach, the main features of particle production at high energy remain universal and are controlled by the saturation scale. This picture has been successfully applied to many QCD processes from HERA to RHIC [3] and the LHC [4–11]. In this paper, we will employ the CGC formalism and show that the semi-inclusive photon-hadron ($\gamma - h$) production processes in pA collisions, i.e., $p + A \to \gamma + h + X$, offer more interesting insights to the dynamics of gluon saturation.

Photons radiated in hard collisions not via hadronic decays are usually called prompt photon. There are advantages to studying prompt photon production as compared to hadron production. It is theoretically cleaner; one avoids the difficulties involved with the description of hadronization and possible initial-state-final-state interference effects which may be present for hadron production and it can be therefore used as a baseline to interpret jet-quenching phenomenon in heavy-ion collisions. A detailed study of Ref. [12] showed that prompt photon production in proton-nucleus (pA) collisions at RHIC and the LHC at forward rapidities is a sensitive probe of the small-x physics and QCD gluon saturation. On the same line, the semi-inclusive prompt photon-hadron production in pA collisions also has advantages over a similar production of dihadron. In particular, in dihadron production, a higher number of Wilson lines and the Weizsäcker-Williams and the dipole gluon distributions are involved [13], while in the photon-hadron production cross section, only dipole gluon distribution appears [12,14], which is both experimentally and theoretically well known; see, for example, Refs. [3,15–21].

Two-particle correlations in high-energy collisions have played a significant role to reveal QCD novel phenomena [22–24]. In particular, the photon-hadron jet correlations have been a very powerful probe of the in-medium parton energy loss in high-energy heavy-ion collisions [24,25]. It was suggested in Ref. [12] that the correlation of the back-to-back photon-hadron pair production in high-energy proton-proton (pp) and pA collisions can be used to probe the gluon saturation at the small-x region and to study the physics of cold nuclear matter in the dense region. However, the correlation defined in Ref. [12] may depend crucially on the so-called underlying event and might be rather challenging to measure. Moreover, in Ref. [12] the correlation was studied in a very limited kinematics; see Sec. IV. In this paper, for the first time we study the coincident probability for photon-hadron correlation at RHIC and the LHC in both pp and pA collisions. Dihadron azimuthal angle correlation was already measured by the coincidence probability at RHIC [23]. We show that the away-side correlations for a pair of photon-hadron obtained via the coincident probability have a

double- or a single-peak structure depending on kinematics and whether the trigger particle is selected to be a prompt photon or hadron. We obtain kinematics conditions for appearance of a double or a single-peak structure for the away-side photon-hadron correlations, which can be verified by the upcoming experiments at RHIC and the LHC. This novel feature is unique for prompt-hadron production in contrast to dihadron production [13], where the trigger particle can only be a hadron and it was already observed at RHIC [23] that the away-side correlation has only single-peak structure. The asymmetric nature of photon-hadron production, and the fact that in semi-inclusive photon-hadron production, QCD and electromagnetic interaction are inextricably intertwined, make the azimuthal correlation of the produced photon hadron very intriguing.

We will also provide quantitative predictions for the (two-dimensional) nuclear modification factor for the semi-inclusive photon-hadron production in pA collisions, and the ratio of single inclusive prompt-photon to hadron production in pp and pA collisions, at RHIC and the LHC at forward rapidities.

This paper is organized as follows: In Sec. II, we first provide a concise description of theoretical framework by introducing the main formulas for the calculation of the cross sections of semi-inclusive photon hadron (Sec. II A), single inclusive prompt photon (Sec. II B), and single inclusive hadron (Sec. II C) production within the CGC approach. In Sec. II D, we describe how to compute the main ingredient of our formalism, namely, dipole-target forward scattering amplitude via the running-coupling Balitsky-Kovchegov evolution equation [15]. In Sec. III, we introduce the observables that we are interested to compute and our numerical setup. In Sec. IV, we present our detailed results and predictions. We summarize our main results in Sec. V.

II. THEORETICAL FRAMEWORK

A. Semi-inclusive prompt photon-hadron production in pp and pA collisions

The cross section for production of a prompt photon and a quark with 4-momenta p^γ and l, respectively, in scattering of a on shell quark with 4-momentum k on a dense target either proton (p) or nucleus (A) at the leading twist approximation in the CGC formalism is given by [14]

$$\frac{d\sigma^{qA\to q(l)\gamma(p^\gamma)X}}{d^2\vec{b}_T d^2\vec{p}_T^{\,\gamma} d^2\vec{l}_T d\eta_\gamma d\eta_h} = \frac{e_q^2\alpha_{em}}{\sqrt{2}(4\pi^4)}\frac{p^-}{(p_T^\gamma)^2\sqrt{S}}\frac{1+(\frac{l^-}{k^-})^2}{[p^-\vec{l}_T - l^-\vec{p}_T^{\,\gamma}]^2}\delta\left[x_q - \frac{l_T}{\sqrt{S}}e^{\eta_h} - \frac{p_T^\gamma}{\sqrt{S}}e^{\eta_\gamma}\right] \times [2l^- p^-\vec{l}_T\cdot\vec{p}_T^{\,\gamma} + p^-(k^- - p^-)l_T^2 + l^-(k^- - l^-)(p_T^\gamma)^2]N_F(|\vec{l}_T + \vec{p}_T^{\,\gamma}|, x_g), \quad (1)$$

where $\sqrt{S}$ is the nucleon-nucleon center of mass energy and the light cone fraction x_q is the ratio of the incoming quark to nucleon energies, namely, $x_q = k^-/\sqrt{S/2}$. The pseudorapidities of outgoing prompt photon η_γ and quark η_h are defined via $p^- = \frac{p_T^\gamma}{\sqrt{2}}e^{\eta_\gamma}$ and $l^- = \frac{l_T}{\sqrt{2}}e^{\eta_h}$. The subscript T stands for the transverse component. The vector $\vec{b}_T$ denotes the impact parameter of interaction. The angle between the final-state quark and prompt photon is denoted by $\Delta\phi$ and defined via $\cos(\Delta\phi) \equiv \frac{\vec{l}_T\cdot\vec{p}_T^{\,\gamma}}{l_t p_T^\gamma}$. Throughout this paper, we only consider light hadron production, therefore at high transverse momentum (ignoring hadron mass), the rapidity, and pseudorapidity is the same. Note that due to the assumption of collinear fragmentation of a quark into a hadron, the angle $\Delta\phi$ is then the angle between the produced photon and hadron, assuming that the rapidity of the parent parton and the fragmented hadron is the same. In Eq. (1), $N_F(p_T, x_g)$ is the imaginary part of (quark-antiquark) dipole-target forward scattering amplitude which satisfies the Jalilian-Marian-Iancu-McLerran-Weigert-Leonidov-Kovner (JIMWLK) evolution equation [26,27] and has all the multiple scattering and small-x evolution effects encoded (see Sec. II D).

In order to relate the above partonic production cross section to proton-target collisions, one needs to convolute the partonic cross section in Eq. (1) with the quark and antiquark distribution functions of a proton and the quark-hadron fragmentation function,

$$\frac{d\sigma^{pA\to h(p^h)\gamma(p^\gamma)X}}{d^2\vec{b}_T d^2\vec{p}_T^{\,\gamma} d^2\vec{p}_T^{\,h} d\eta_\gamma d\eta_h} = \int_{z_f^{\min}}^1 \frac{dz_f}{z_f^2}\int dx_q f_q(x_q, Q^2)\frac{d\sigma^{qA\to q(l)\gamma(p^\gamma)X}}{d^2\vec{b}_T d^2\vec{p}_T^{\,\gamma} d^2\vec{l}_T d\eta_\gamma d\eta_h} \times D_{h/q}(z_f, Q^2), \quad (2)$$

where p_T^h is the transverse momentum of the produced hadron, and $f_q(x_q, Q^2)$ is the parton (quark) distribution function (PDF) of the incoming proton which depends on the light cone momentum fraction x_q and the hard scale Q. A summation over the quark and antiquark flavors in the above expression should be understood. The function $D_{h/q}(z_f, Q)$ is the quark-hadron fragmentation function (FF), where z_f is the ratio of energies of the produced hadron and quark.

The light cone momentum fraction x_q, $x_{\bar{q}}$, x_g in Eqs. (1) and (2) are related to the transverse momenta

and rapidities of the produced hadron and prompt photon via (see the Appendix in Ref. [12])

$$x_q = x_{\bar{q}} = \frac{1}{\sqrt{S}}\left(p_T^\gamma e^{\eta_\gamma} + \frac{p_T^h}{z_f} e^{\eta_h}\right),$$
$$x_g = \frac{1}{\sqrt{S}}\left(p_T^\gamma e^{-\eta_\gamma} + \frac{p_T^h}{z_f} e^{-\eta_h}\right), \tag{3}$$
$$z_f = p_T^h/l_T, \quad \text{with} \quad z_f^{\min} = \frac{p_T^h}{\sqrt{S}}\left(\frac{e^{\eta_h}}{1 - \frac{p_T^\gamma}{\sqrt{S}} e^{\eta_\gamma}}\right).$$

B. Single inclusive prompt photon production in pp and pA collisions

The prompt photon cross section in the CGC framework can be readily obtained from Eq. (1) by integrating over the momenta of the final-state quark. After some algebra, the single inclusive prompt photon production can be divided into two contributions of fragmentation and direct photon [12],

$$\frac{d\sigma^{qA\to\gamma(p^\gamma)X}}{d^2\vec{b}_T d^2\vec{p}_T^\gamma d\eta_\gamma} = \frac{d\sigma^{\text{Fragmentation}}}{d^2\vec{b}_T d^2\vec{p}_T^\gamma d\eta_\gamma} + \frac{d\sigma^{\text{Direct}}}{d^2\vec{b}_T d^2\vec{p}_T^\gamma d\eta_\gamma},$$
$$= \frac{1}{(2\pi)^2}\frac{1}{z} D_{\gamma/q}(z, Q^2) N_F(x_g, p_T^\gamma/z)$$
$$+ \frac{e_q^2 \alpha_{em}}{\pi(2\pi)^3} z^2[1 + (1-z)^2]\frac{1}{(p_T^\gamma)^4}$$
$$\times \int_{l_T^2 < Q^2} d^2\vec{l}_T l_T^2 N_F(\bar{x}_g, l_T), \tag{4}$$

where p_T^γ is the transverse momentum of the produced prompt photon, and $D_{\gamma/q}(z, Q^2)$ is the leading order quark-photon fragmentation function [28]. In order to relate the partonic cross section given by Eq. (4) to prompt photon production in pA collisions, we convolute Eq. (4) with quark and antiquark distribution functions of the projectile proton [29],

$$\frac{d\sigma^{pA\to\gamma(p^\gamma)X}}{d^2\vec{b}_T d^2\vec{p}_T^\gamma d\eta_\gamma} = \int_{x_q^{\min}}^1 dx_q f_q(x_q, Q^2) \frac{d\sigma^{q(q^h)A\to\gamma(p^\gamma)X}}{d^2\vec{b}_T d^2\vec{p}_T^\gamma d\eta_\gamma}, \tag{5}$$

where a summation over different quarks (antiquarks) flavors is implicit. The light cone fraction variables x_g, $\bar{x}_g$, z in Eqs. (4) and (5) are related to the transverse momentum of the produced prompt photon and its rapidity [12],

$$x_g = \frac{(p_T^\gamma)^2}{z^2 x_q S} = x_q e^{-2\eta_\gamma},$$
$$\bar{x}_g = \frac{1}{x_q S}\left[\frac{(p_T^\gamma)^2}{z} + \frac{(l_T - p_T^\gamma)^2}{1-z}\right],$$
$$z \equiv \frac{p^-}{q^-} = \frac{p_T^\gamma}{x_q\sqrt{S}} e^{\eta_\gamma} = \frac{x_q^{\min}}{x_q}, \quad \text{with} \tag{6}$$
$$x_q^{\min} = z_{\min} = \frac{p_T^\gamma}{\sqrt{S}} e^{\eta_\gamma}.$$

C. Single inclusive hadron production in pp and pA collisions

The cross section for single inclusive hadron production at leading twist approximation, in asymmetric collisions such as pA or forward rapidity pp collisions at high energy, in the CGC formalism is given by [30,31]

$$\frac{dN^{pA\to hX}}{d^2\vec{p}_T^h d\eta_h}$$
$$= \frac{1}{(2\pi)^2}\left[\int_{x_F}^1 \frac{dz}{z^2}\left[x_1 f_g(x_1, Q^2) N_A\left(x_2, \frac{p_T^h}{z}\right) D_{h/g}(z, Q^2)\right.\right.$$
$$\left.\left. + \Sigma_q x_1 f_q(x_1, Q^2) N_F\left(x_2, \frac{p_T^h}{z}\right) D_{h/q}(z, Q^2)\right] + \delta^{\text{inelastic}}\right], \tag{7}$$

where the variables η_h and p_T^h are the pseudorapidity and transverse momentum of the produced hadron. The functions f_q, $N_{F(A)}$ and $D_{h/q}$ in the above are defined the same as in Eq. (2). The indices q and g denote quarks and gluons, with a summation over different flavors being implicit. The first two terms in the above expression correspond to elastic contribution, namely, an incoming parton scattering elastically with the CGC target [30]. This incoming parton with initial zero transverse momentum picks up transverse momentum of an order saturation scale after multiply scattering on the target. There is also inelastic contribution to the cross section denoted by $\delta^{\text{inelastic}}$ corresponding to a high transverse momentum parton radiated from the incoming parton in the projectile wave function [31,32]. In this case, the projectile parton interacts with the target with small transfer momentum exchanges, but this is enough to decohere the preexisting high-p_T parton from the hadron wave function and release it as an on shell particle. The high-p_T partons in the projectile wave function arise due to Dokshitzer-Gribov-Lipatov-Altarelli-Parisi splitting of partons. It was shown in Ref. [32] that at very forward rapidities the inelastic contributions are less important compared to elastic ones while it is significant at midrapidity at high-energy scatterings.

The longitudinal momentum fractions x_1 and x_2 are defined as follows:

$$x_F \approx \frac{p_T^h}{\sqrt{S}} e^{\eta_h}, \qquad x_1 = \frac{x_F}{z}, \qquad x_2 = x_1 e^{-2\eta_h}. \tag{8}$$

One should note that the light cone fraction variables defined above for the inclusive hadron production are different from the corresponding light cone variables for single inclusive prompt photon Eq. (6) and semi-inclusive photon-hadron Eq. (3) production.

D. Small-x evolution equation and the dipole forward scattering amplitude

The main ingredient in the cross section of semi-inclusive photon-hadron production in Eq. (1), single inclusive prompt photon production in Eq. (4), and single inclusive hadron production in Eq. (7) is the universal dipole forward scattering amplitude which incorporates small-x dynamics and can be calculated via the first-principle nonlinear JIMWLK equations [26,27]. In Eqs. (1), (4), and (7), the amplitude N_F (N_A) is the two-dimensional Fourier transformed of the imaginary part of the forward dipole-target scattering amplitude $\mathcal{N}_{A(F)}$ in the fundamental (F) or adjoint (A) representation,

$$N_{A(F)}(x, k_T) = \int d^2\vec{r} e^{-i\vec{k}_T\cdot\vec{r}}(1 - \mathcal{N}_{A(F)}(r, Y = \ln(x_0/x))), \tag{9}$$

where $r = |\vec{r}|$ is the dipole transverse size. In the large-N_c limit, one has the following relation between the adjoint and fundamental dipoles:

$$\mathcal{N}_A(r, Y) = 2\mathcal{N}_F(r, Y) - \mathcal{N}_F^2(r, Y). \tag{10}$$

In the large N_c limit, the coupled JIMWLK equations are simplified to the Balitsky-Kovchegov (BK) equation [15–18], a closed-form equation for the rapidity evolution of the dipole amplitude in which both linear radiative processes and nonlinear recombination effects are systematically incorporated. The running-coupling BK (rcBK) equation has the following simple form:

$$\frac{\partial \mathcal{N}_{A(F)}(r, x)}{\partial \ln(x_0/x)} = \int d^2\vec{r}_1 K^{\text{run}}(\vec{r}, \vec{r}_1, \vec{r}_2)[\mathcal{N}_{A(F)}(r_1, x) + \mathcal{N}_{A(F)}(r_2, x) - \mathcal{N}_{A(F)}(r, x) - \mathcal{N}_{A(F)}(r_1, x)\mathcal{N}_{A(F)}(r_2, x)], \tag{11}$$

where the evolution kernel K^{run} using Balitsky's prescription [16] for the running coupling is defined as

$$K^{\text{run}}(\vec{r}, \vec{r}_1, \vec{r}_2) = \frac{N_c \alpha_s(r^2)}{2\pi^2}\left[\frac{1}{r_1^2}\left(\frac{\alpha_s(r_1^2)}{\alpha_s(r_2^2)} - 1\right) + \frac{r^2}{r_1^2 r_2^2} + \frac{1}{r_2^2}\left(\frac{\alpha_s(r_2^2)}{\alpha_s(r_1^2)} - 1\right)\right], \tag{12}$$

with $\vec{r}_2 \equiv \vec{r} - \vec{r}_1$. The only external input for the rcBK nonlinear equation is the initial condition for the evolution which is taken to have the following form motivated by the McLerran-Venugopalan model [2]:

$$\mathcal{N}(r, Y = 0) = 1 - \exp\left[-\frac{(r^2 Q_{0s}^2)^\gamma}{4}\ln\left(\frac{1}{\Lambda r} + e\right)\right], \tag{13}$$

where the infrared scale is taken $\Lambda = 0.241$ GeV and the onset of small-x evolution is assumed to be at $x_0 = 0.01$ [19]. The only free parameters in the above are γ and the initial saturation scale Q_{0s} (probed by quarks), with a notation $s = p$ and, A for a proton and nuclear target, respectively. The initial saturation scale of proton $Q_{0p}^2 \simeq 0.168$ GeV^2 with the corresponding $\gamma \simeq 1.119$ were extracted from a global fit to proton structure functions in deep inelastic scattering (DIS) in the small-x region [19] and single inclusive hadron data in pp collisions at RHIC and the LHC [8,32–34]. Note that the current HERA data alone is not enough to uniquely fix the values of Q_{0p} and γ [19]. The recent LHC data, however, seems to indicate that $\gamma > 1$ is preferable [8]. We will consider the uncertainties coming from our freedom to choose among different parameter sets for the rcBK description of the proton.

Notice that in the rcBK equation, Eq. (11), the impact-parameter dependence of the collisions was ignored. Solving the rcBK equation in the presence of the impact parameter is still an open problem [35]. However, for the minimum-bias analysis considered here this may not be important. Then, the initial saturation scale of a nucleus Q_{0A} should be considered as an impact-parameter averaged value and it is extracted from the minimum-bias data. For the minimum-bias collisions, one may assume that the initial saturation scale of a nucleus with atomic mass number A, scales linearly with $A^{1/3}$ [2], namely, we have $Q_{0A}^2 = cA^{1/3}Q_{0p}^2$ where the parameter c is fixed from a fit to data.[1] In Ref. [34], it was shown that DIS data for heavy nuclear targets can be described with $c \approx 0.5$. This is consistent with the fact that RHIC inclusive hadron production data in minimum-bias deuteron-gold collisions prefers an initial saturation scale within $Q_{0A}^2 \approx 3 \div 4Q_{0p}^2$ [32,33]. We will take into account the uncertainties associated with the variation of the initial saturation scale in the rcBK evolution equation.

III. OBSERVABLES AND NUMERICAL SETUP

In this paper, we only consider observables which are defined as a ratio of cross sections. We expect that some of the theoretical uncertainties, such as sensitivity to K factors which effectively incorporates the missing higher order corrections, will drop out in this way. Therefore, we take $K = 1$ throughout this paper. We start by considering

[1]Note that a different A dependence of the nuclear saturation scale with a prefactor fitted to the HERA data, numerically leads to a very similar relation between the proton and nuclear saturation scale [36].

the ratio of inclusive prompt photon to the neutral pion production, defined as

$$\frac{\gamma^{\rm inclusive}}{\pi^0}(p_T^\gamma, p_T^h; \eta_h, \eta_\gamma) = \frac{dN^{pA\to\gamma(p_T^\gamma)X}}{d^2\vec{p}_T^{\,\gamma} d\eta_\gamma} \Big/ \frac{dN^{pA\to h(p_T^h)X}}{d^2\vec{p}_T^{\,h} d\eta_h}, \tag{14}$$

where the cross section for the single inclusive prompt photon and hadron production in pA and pp collisions are given in Eqs. (5) and (7).

In order to investigate the azimuthal angle correlations between the produced prompt photon and hadron, we calculate the coincidence probability. In the contrast to a more symmetric production like dihadron, for the photon-hadron production we have freedom to select the trigger particle to be a produced prompt photon or a hadron. We consider here both cases. In a case that the trigger particle is a prompt photon, the coincidence probability is defined as $CP_h(\Delta\phi) = N_h^{\rm pair}(\Delta\phi)/N_{\rm photon}$, where $N_h^{\rm pair}(\Delta\phi)$ is the yield of photon-hadron pair production including a associated hadron (neutral pion) with a transverse momentum $p_{T,S}^h$ with a trigger (leading) prompt photon with transverse momentum $p_{T,L}^\gamma$ and the azimuthal angle between them $\Delta\phi$. In the same fashion, one can define the coincidence probability with a hadron triggered as $CP_\gamma(\Delta\phi) = N_\gamma^{\rm pair}(\Delta\phi)/N_{\rm hadron}$, where $N_\gamma^{\rm pair}(\Delta\phi)$ is the yield of photon-hadron pair including a associated prompt photon and a trigger hadron (neutral pion) with transverse momentum denoted by $p_{T,S}^\gamma$ and $p_{T,L}^h$, respectively,

$$CP_h(\Delta\phi; p_{T,S}^h, p_{T,L}^\gamma; \eta_\gamma, \eta_h) = \frac{2\pi \int_{p_{T,L}^\gamma} dp_T^\gamma p_T^\gamma \int_{p_{T,S}^h} dp_T^h p_T^h \frac{dN^{pA\to h(p_T^h)\gamma(p_T^\gamma)X}}{d^2\vec{p}_T^{\,\gamma} d^2\vec{p}_T^{\,h} d\eta^\gamma d\eta^h}}{\int_{p_{T,L}^\gamma} d^2\vec{p}_T^{\,\gamma} \frac{dN^{pA\to\gamma(p_T^\gamma)X}}{d^2\vec{p}_T^{\,\gamma} d\eta_\gamma}}, \tag{15}$$

$$CP_\gamma(\Delta\phi; p_{T,S}^\gamma, p_{T,L}^h; \eta_\gamma, \eta_h) = \frac{2\pi \int_{p_{T,L}^h} dp_T^h p_T^h \int_{p_{T,S}^\gamma} dp_T^\gamma p_T^\gamma \frac{dN^{pA\to h(p_T^h)\gamma(p_T^\gamma)X}}{d^2\vec{p}_T^{\,\gamma} d^2\vec{p}_T^{\,h} d\eta^\gamma d\eta^h}}{\int_{p_{T,L}^h} d^2\vec{p}_T^{\,h} \frac{dN^{pA\to h(p_T^h)X}}{d^2\vec{p}_T^{\,h} d\eta_h}}, \tag{16}$$

where the integrals are performed within given momenta bins denoted by subscript $p_{T,L}^\gamma$, $p_{T,S}^\gamma$, $p_{T,L}^h$, and $p_{T,S}^h$. The yields in the above expression are defined in Eqs. (1), (4), and (7). Similar to the dihadron correlation measurements at RHIC [23], in the definition of the coincidence probability, we follow a convention that a leading or trigger particle has transverse momentum *larger* than an associated particle. Later, we will also study, the implication of different kinematic definitions for the trigger particle in $\gamma - h$ correlations.

In nuclear collisions, nuclear effects on particle production may be evaluated in terms of ratios of particle yields in pA and pp collisions (scaled with a proper normalization), the so-called nuclear modification factor R_{pA}. The nuclear modification factor for semi-inclusive photon-hadron production is defined as

$$R_{pA}^{h\gamma}(\Delta\phi; p_T^h, p_T^\gamma; \eta_\gamma, \eta_h) = \frac{1}{N_{\rm coll}} \frac{dN^{pA\to h(p_T^h)\gamma(p_T^\gamma)X}}{d^2\vec{p}_T^{\,h} d^2\vec{p}_T^{\,\gamma} d\eta_\gamma d\eta_h} \Big/ \frac{dN^{pp\to h(p_T^h)\gamma(p_T^\gamma)X}}{d^2\vec{p}_T^{\,h} d^2\vec{p}_T^{\,\gamma} d\eta_\gamma d\eta_h}, \tag{17}$$

$$R_{pA}^{h\gamma}(p_T^h, p_T^\gamma; \eta_\gamma, \eta_h) = \frac{1}{N_{\rm coll}} \frac{dN^{pA\to h(p_T^h)\gamma(p_T^\gamma)X}}{dp_T^h dp_T^\gamma d\eta_\gamma d\eta_h} \Big/ \frac{dN^{pp\to h(p_T^h)\gamma(p_T^\gamma)X}}{dp_T^h dp_T^\gamma d\eta_\gamma d\eta_h}, \tag{18}$$

where the photon-hadron yield in high-energy pA and pp collisions is given in Eq. (1). In Eq. (18), the integrals over the angles were performed. The normalization constant $N_{\rm coll}$ is the number of binary proton-nucleus collisions. We take $N_{\rm coll} = 3.6$ and 7.4 at $\sqrt{s} = 0.2$ and 8.8 TeV, respectively, in pA collisions [37]. Notice that in our approach $N_{\rm coll}$ is taken from the outset and one should take into account a possible discrepancy between our assumed normalization $N_{\rm coll}$ and the experimentally measured value for $N_{\rm coll}$ by rescaling our curves.

We will use the next to leading order Martin-Stirling-Thorne-Watt 2008 PDFs [38] and the next to leading order Kniehl-Kramer-Potter FFs [39] for neutral pion. For the photon fragmentation function, we will use the full leading log parametrization [28,40]. We assume the factorization scale Q in the FFs and the PDFs to be equal and its value is taken to be p_T^h and p_T^γ for inclusive (and semi-inclusive) hadron and prompt photon production, respectively.

IV. MAIN RESULTS AND PREDICTIONS

In Fig. 1 (right), we show the ratio of single inclusive prompt photon to neutral pion (π^0) production defined via Eq. (14) for $\eta_h = \eta_\gamma = \eta$ and $p_T^\gamma = p_T^h = p_T$ at the LHC energy $\sqrt{S} = 8.8$ TeV as a function of transverse momentum p_T in minimum-bias pp and pA collisions at different rapidities η. It is seen that at the LHC, the ratio $\gamma^{\rm inclusive}/\pi^0$ is smaller than one for a large range of rapidities. In Fig. 1 (left), we compare the ratio $\gamma^{\rm inclusive}/\pi^0$ at a fixed rapidity $\eta = 3$ but different energies. In our approach, a fast valence quark from the projectile proton radiates a photon before and after multiply interaction on the color-glass-condensate target [12]. The prompt photon can be mainly produced by quark (at the leading log approximation), while pions can be produced by both projectile gluons and quarks; see Eqs. (5) and (7). At the LHC energies at around midrapidity, gluons dominate and consequently the pion production rate is higher than prompt photon while for forward collisions and hight p_T we have $x_1 \to 1$, therefore *projectile* quark distributions enhance and consequently the prompt photon production rate grows with increasing rapidity. This can be seen from Fig. 1, namely, the ratio $\gamma^{\rm inclusive}/\pi^0$ increases with rapidity and transverse momentum while it decreases with

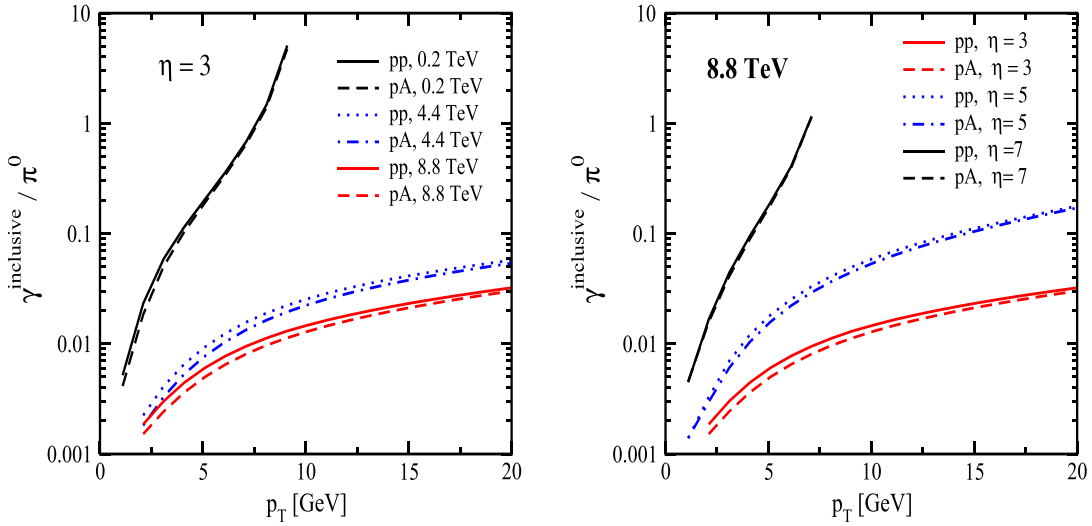

FIG. 1 (color online). The ratio $\gamma^{\text{inclusive}}/\pi^0$ as a function of transverse momentum $p_T^\gamma = p_T^h = p_T$ at various rapidities $\eta_h = \eta_\gamma = \eta$ and energies in minimum bias pp and pA collisions.

energy. Note that in our picture, the description of the target appears via the dipole-target forward scattering amplitude and it numerically drops out in the ratio, and as a consequence the ratio $\gamma^{\text{inclusive}}/\pi^0$ is approximately equal for pp and pA collisions at high p_T and is not sensitive to the initial saturation scale.[2]

Next, we study the azimuthal angle correlation of photon-hadron $(\gamma - \pi^0)$ production by computing the coincidence probability defined in Eqs. (15) and (16). In Figs. (2 and 3) we show the coincidence probability for photon-hadron production at RHIC and the LHC energy at various kinematics obtained by solutions of the rcBK evolution equation (11) with a initial saturation scale for proton $Q_{0p}^2 = 0.168\ \text{GeV}^2$ and for a nucleus within $Q_{0A}^2 = 3 \div 4Q_{0p}^2$ (corresponding to the band). It is seen that the away-side correlation has a double- or single-peak structure depending on the definition of the trigger (or the leading particle) and kinematics. Namely, if the leading particle is selected, a prompt photon with $p_T^\gamma \geq p_T^h$, then the corresponding coincidence probability $CP_h(\Delta\phi)$ defined via Eq. (15), can have a double-peak structure at $\Delta\phi = \pi$. But if the leading particle is selected to be a hadron with $p_T^h > p_T^\gamma$, then the coincidence probability $CP_\gamma(\Delta\phi)$ defined via Eq. (16), has a single-peak structure at $\Delta\phi = \pi$. In order to understand this phenomenon, first note that the cross section of semi-inclusive photon-hadron production in quark-nucleus collisions given by Eq. (1), becomes zero for

$$p_T = |\vec{l}_T + \vec{p}_T^\gamma| = 0. \tag{19}$$

[2]Note that in calculation of the ratio of $\gamma^{\text{inclusive}}/\pi^0$ we ignored the inelastic contributions in both inclusive prompt photon and hadron production cross sections assuming that higher order terms will be canceled out in the ratio.

This is simply because if the projectile parton is already without any transverse momentum, the production rate of photon hadron should go to zero and the off shell photon remains as part of the projectile hadron wave function. In other words, in order for the higher Fock components of the projectile hadron wave function to be resolved and a photon to be radiated, the projectile quark should interact with small-x target via exchanging transverse momentum. The necessary kinematics for having a local minimum for the cross section of photon-hadron production can be readily obtained from Eq. (19) by using relations given in Eq. (3), namely, $l_T = p_T^h/z_f$ and the fact that for the fragmentation fraction we have $z_f^{\min} \leq z_f \leq 1$. Therefore, we obtain

$$z_T = \frac{p_T^h}{p_T^\gamma} \leq 1, \tag{20}$$

$$p_T^\gamma \frac{(e^{\eta_h} + e^{\eta_\gamma})}{\sqrt{S}} \leq 1. \tag{21}$$

Note that in our approach, the projectile is treated in the collinear factorization [14]. Therefore, radiation of the photon from quark at this level has the standard features of pQCD, including the back-to-back correlation in the transverse momentum. Moreover, due to multiple scatterings with target, the cross section of photon-hadron production should have a local minimum for the back-to-back production provided the kinematics conditions given in Eqs. (20) and (21) are satisfied. However, because of convolution with fragmentation and parton distribution functions, the local minimum will not be zero, but gets smeared out. On the other hand, the product of $p_T^2 N_F(p_T, x_g)$ in Eq. (1) has a maximum when the transverse momentum p_T approaches the

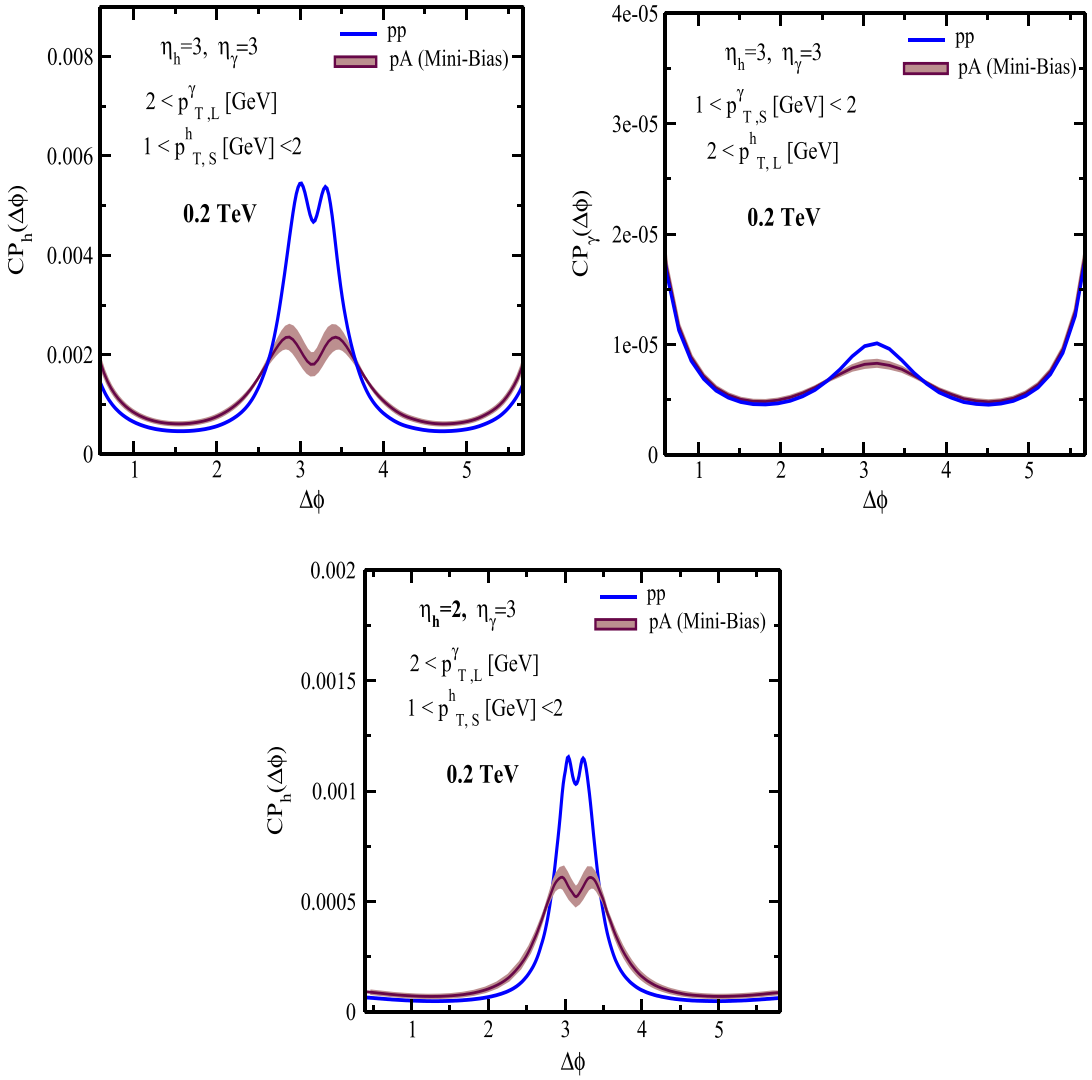

FIG. 2 (color online). The photon-hadron ($\gamma - \pi^0$) azimuthal correlation (the coincidence probability) $CP_h(\Delta\phi)$ and $CP_\gamma(\Delta\phi)$ defined in Eqs. (15) and (16) in minimum-bias (mini-bias) pA and pp collisions at RHIC $\sqrt{S} = 0.2$ TeV at different rapidities for the produced hadron η_h and inclusive prompt photon η_γ. In the plot, the values of transverse momenta bins of the associated (and leading) neutral pion $p^h_{T,S}$ (and $p^h_{T,L}$) and leading (and associated) prompt photon $p^\gamma_{T,L}$ (and $p^\gamma_{T,S}$) are given.

saturation scale. As a result, a double-peak structure appears for the away-side correlation. Note that the integrand in the coincidence probability samples smaller transverse momentum for photon than hadron for the same reason we already mentioned, namely, a photon can be produced if the parton already acquired a transverse momentum impulse. In the case that the trigger particle is selected to be a hadron rather than a prompt photon, one should perform the integral over the transverse momentum of the hadron, which is larger than transverse momentum of photon $z_T > 1$, violating the condition given in Eq. (20), and consequently the local minimum at $\Delta\phi = \pi$ is washed away and as a result the double-peak structure will be fused to a single peak. This can be clearly seen in Figs. (2 and 3) at both RHIC and the LHC.

In order to further investigate the consequences of the conditions given in Eqs. (20) and (21), let us defined the azimuthal correlation in the following form [12],

$$P(\Delta\phi) = \frac{d\sigma^{pA\to h(p_T^h)\gamma(p_T^\gamma)X}}{d^2\vec{b}_t p_T^h dp_T^h p_T^\gamma dp_T^\gamma d\eta_\gamma d\eta_h d\phi}[\Delta\phi] \Big/ \frac{d\sigma^{pA\to h(p_T^h)\gamma(p_T^\gamma)X}}{d^2\vec{b}_t p_T^h dp_T^h p_T^\gamma dp_T^\gamma d\eta_\gamma d\eta_h d\phi}[\Delta\phi = \Delta\phi_c], \tag{22}$$

which has the meaning of the probability of the semi-inclusive photon-hadron pair production at a certain kinematics and angle $\Delta\phi$, triggering the same production with the same kinematics at a fixed reference angle $\Delta\phi_c = \pi/2$. The correlation defined in Eq. (22) may be

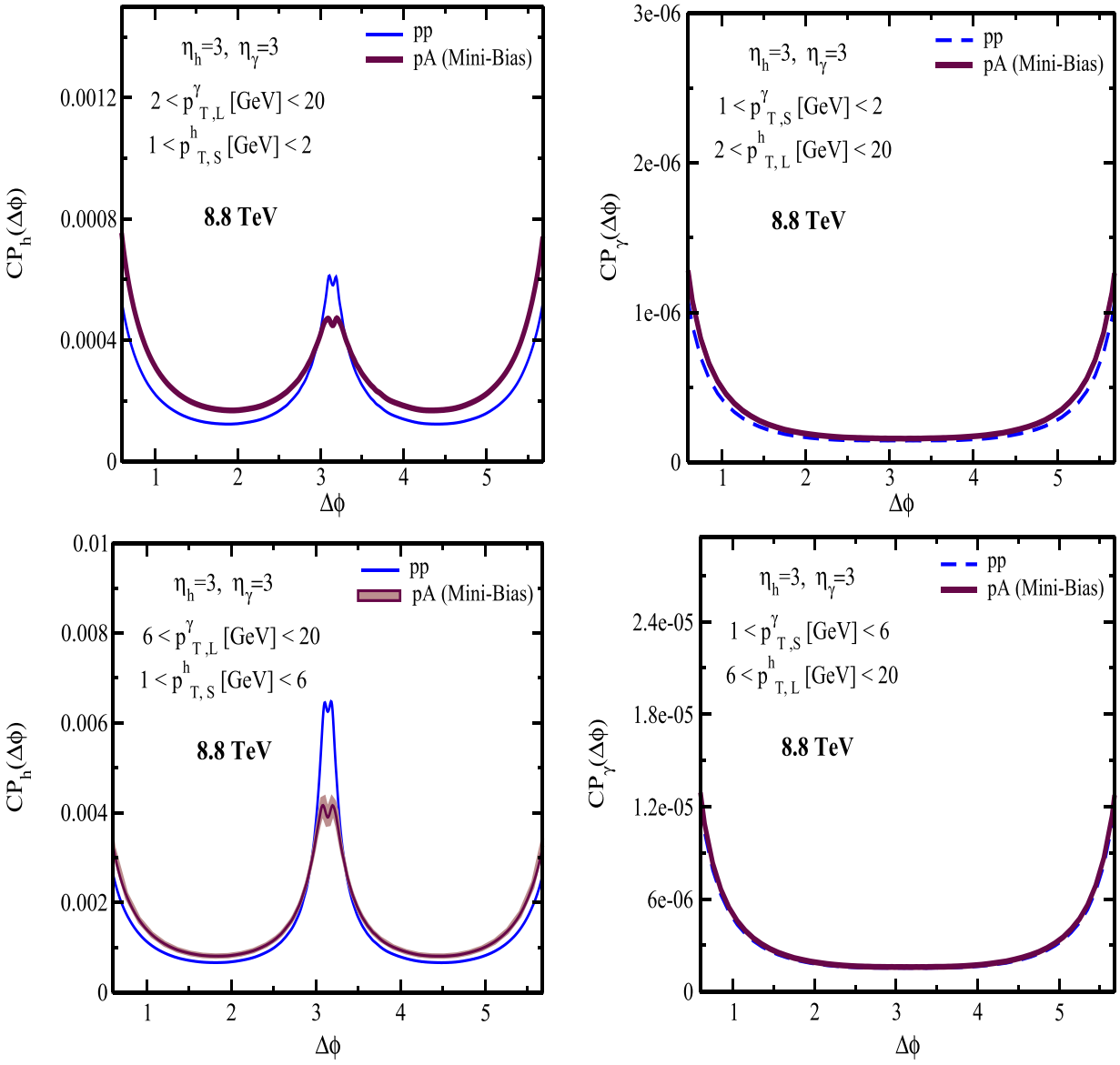

FIG. 3 (color online). The $\gamma - \pi^0$ coincidence probability $CP_h(\Delta\phi)$ and $CP_\gamma(\Delta\phi)$ in minimum-bias pA and pp collisions at the LHC $\sqrt{S} = 8.8$ TeV at $\eta_h = \eta_\gamma = 3$ for two bins of transverse momenta of the associated (and leading) neutral pion $p^h_{T,S}$ (and $p^h_{T,L}$) and leading (and associated) prompt photon $p^\gamma_{T,L}$ (and $p^\gamma_{T,S}$).

more challenging to measure compared to the coincidence probability defined in Eqs. (15) and (16), due to the so-called underlying event dependence, but it is free from the extra integrals over transverse momenta and this facilitates to clearly examine the conditions in Eqs. (20) and (21). In a sense, the correlation defined in Eq. (22) can be considered as a snap shot of the integrand in the coincidence probability defined in Eqs. (15) and (16).

In Fig. 4, we show the photon-hadron correlation $P(\Delta\phi)$ defined in Eq. (22) at forward rapidity $\eta_h = \eta_\gamma = 3$ for various transverse momenta of produced prompt photon p^γ_T, and hadron p^h_T at RHIC and the LHC for minimum-bias pA collisions. The initial saturation scale for proton $Q^2_{0p} = 0.168$ GeV^2 and nuclei $Q^2_{0A} = 3Q^2_{0p}$ are fixed for all curves. It is clearly seen that the photon-hadron away-side correlations can have a double-peak structure both at RHIC and the LHC for the kinematics satisfying the conditions in Eqs. (20) and (21), and the away-side double-peak correlations will evolve to a single-peak structure for kinematics outside of region defined by Eqs. (20) and (21).

In high-energy collisions, the produced parton on average have intrinsic transverse momentum of order of the saturation scale. By increasing the energy or density or decreasing the transverse momentum of the probe, the saturation scale Q_s increases and consequently this washes away the intrinsic back-to-back correlations and the

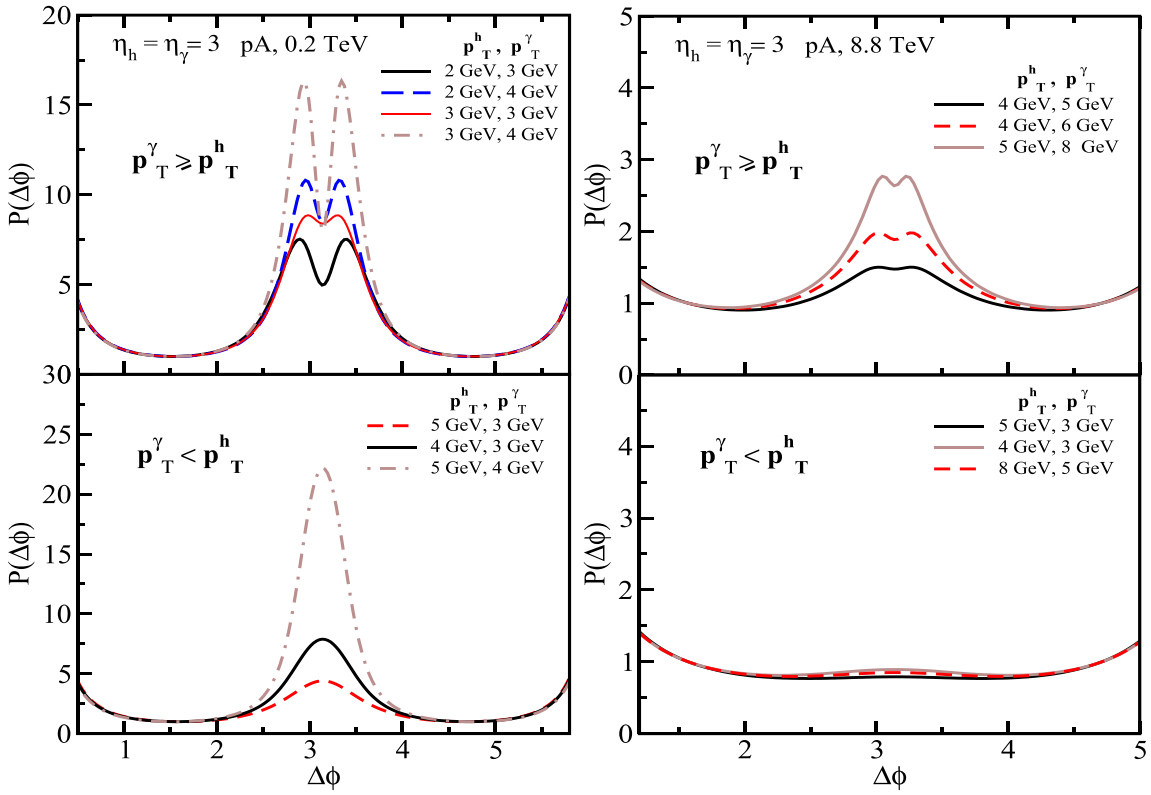

FIG. 4 (color online). The photon-hadron correlation $P(\Delta\phi)$ defined in Eq. (22) in minimum-bias pA collisions at the LHC (right) and RHIC (left) at forward rapidity for various transverse momenta of produced prompt photon p_T^γ and hadron p_T^h corresponding to two cases of $z_T > 1$ and $z_T < 1$.

away-side correlation is suppressed. Numerically, a bigger saturation scale, pushes the unintegrated gluon density profile to larger transverse momentum. As a result, the single inclusive production (either hadron or prompt photon) cross section (the denumenator in the coincidence probability) is enhanced, while the two-particle correlated cross section Eq. (1) is suppressed by a larger saturation scale Q_s. Therefore, the coincidence probability defined in Eqs. (15) and (16) decreases with increasing the saturation scale and we expect the photon-hadron away-side correlation at the LHC to be smaller than RHIC (at the same rapidity and transverse momenta of associated and leading particle). This can be clearly seen in Fig. 5 where we compare the coincidence probability $CP_h(\Delta\phi)$ obtained at various energies. Moreover, the saturation scale grows with density, therefore the away-side correlations in pA collisions should be more suppressed compared to pp collisions at the same kinematics; see Figs. (2 and 3).

It is seen from Figs. (2–4) that generally at a fixed rapidity and energy, the suppression of away-side $\gamma - h$ correlation is larger for a case that $z_T > 1$. This effect can be traced back to the fact that $\gamma - h$ pairs with $z_T > 1$ probe lower x_g region compared to the cases that $z_T < 1$. This can be understood by rewriting the definition of x_g in Eq. (3), which appears in the unintegrated gluon density in terms of x_T, namely, $x_g = \frac{p_T^\gamma}{\sqrt{S}}(e^{-\eta_\gamma} + \frac{z_T}{z_f}e^{-\eta_h})$. Therefore, $\gamma - h$ pair production with $z_T > 1$ have a lower x_g and consequently the suppression due to saturation will be larger.

In Fig. 3, we show $CP_h(\Delta\phi)$ and $CP_\gamma(\Delta\phi)$ at the LHC $\sqrt{S} = 8.8$ TeV at forward rapidity $\eta_h = \eta_\gamma = 3$ in minimum-bias pA and pp collisions for two bins of transverse momenta of associated prompt photon $p_{T,S}^\gamma$ and hadron $p_{T,S}^h$, and the corresponding leading hadron $p_{T,L}^\gamma$ and prompt photon $p_{T,L}^\gamma$. Namely, in the top and lower panel we performed the integral for the associated particle within [1,2] GeV and [1,6] GeV (and for the corresponding leading particle within [2,20] GeV and [6,20] GeV), respectively. The correlation signal enhances by increasing the transverse momenta interval of the associated particle. This is simply because in Eqs. (15) and (16), by construction, the integrals over the leading particle is mainly canceled out in the ratio, and the correlation becomes proportional to the integral over the associated particle. For higher transverse momenta bins, the saturation scale is smaller and the back-to-back correlation is restored. Notice that since the rcBK evolution solution is not reliable at high transverse momentum, we had to impose an upper limit cut

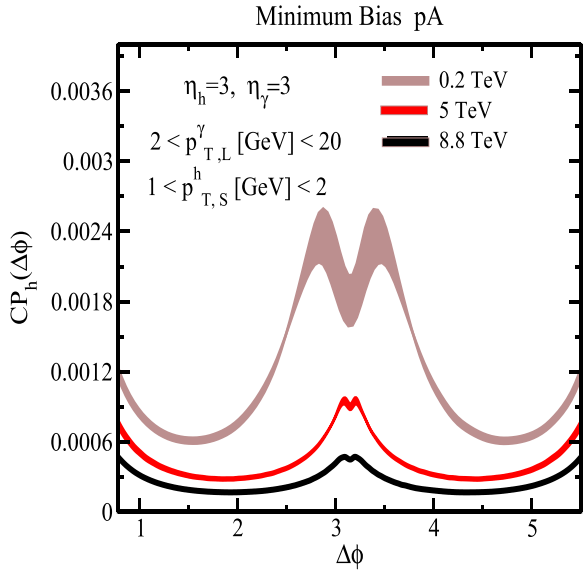

FIG. 5 (color online). The $\gamma - \pi^0$ azimuthal correlation $CP_h(\Delta\phi)$ defined in Eq. (15) in minimum-bias pA collisions at forward rapidity $\eta_h = \eta_\gamma = 3$ for various energies at RHIC and the LHC.

for the integrals over transverse momenta of the leading particle in Eq. (15) and (16). However, the cross sections drop so fast with transverse momentum at forward rapidities that this upper cutoff should not make a big difference.

The azimuthal correlation $CP_h(\Delta\phi)$ defined in Eq. (15) is generally bigger than the corresponding correlation $CP_\gamma(\Delta\phi)$ defined in Eq. (16), at the same kinematics. This is because when the trigger particle is taken a prompt photon, in Eq. (15), the electromagnetic coupling $\alpha_{\rm em}$, drops out in the ratio of two cross sections and that enhances the signal compared to the case that the trigger particle is selected to be a hadron. This can be seen in Figs. (2 and 3).

As we already pointed out, the double-peak structure for the photon-hadron coincidence probability $CP_h(\Delta\phi)$ at $\Delta\phi \approx \pi$ is due to the interplay between a local minimum for the cross section at $p_T \approx 0$ and two maxima for the cross section when $p_T \approx Q_s$. The double-peak structure can be stretched out and becomes more pronounced by measuring the associated hadron at about or higher rapidity than the trigger prompt photon, i.e., $\eta_h \geq \eta_\gamma$. This is due to the fact that because of the kinematic limit for more forward production, the integrand of the associated hadron in $CP_h(\Delta\phi)$ is relatively shifted to lower transverse momentum and consequently the conditions for local minimum in Eqs. (20) and (21) are satisfied while at the same time, the saturation scale increases for more forward production leading to an enhancement of the two local maxima. In Figs. (2 and 6), we show this effect by comparing the azimuthal correlations at different rapidities, η_h and η_γ, at RHIC and the LHC.

Although the main features of the photon-hadron correlations, e.g., the double- or single-peak structure and decorrelation with energy/rapidity, density, and transverse momentum seem to be robust and understandable due to the nonlinear gluon saturation dynamics, there are some uncertainties on the magnitude of the correlation obtained in our approach. These uncertainties are due to the fact that with available worldwide small-x experimental data it is not yet possible to uniquely fix the parameters of the rcBK evolution equation and the initial saturation scale of the proton and nucleus [8,19,32–34]. To highlight our main uncertainties, in Fig. 7 we show $CP_h(\Delta\phi)$ for minimum-bias pA and pp collisions at forward rapidity at RHIC and the LHC, with two different initial saturation scales of proton, namely, $Q^2_{0p} = 0.168$ and 0.2 GeV^2 corresponding

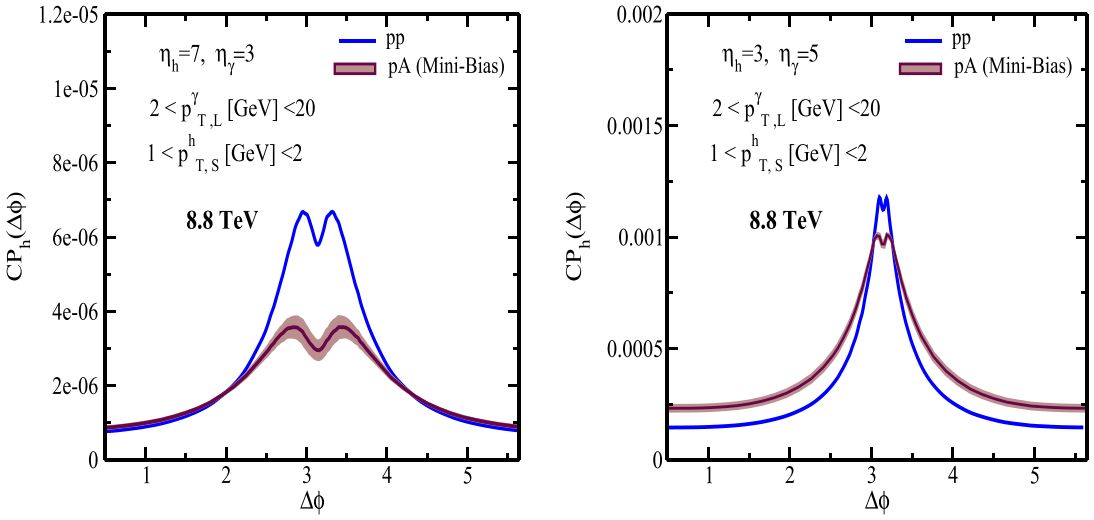

FIG. 6 (color online). The $\gamma - \pi^0$ azimuthal correlation $CP_h(\Delta\phi)$ defined in Eq. (15) in minimum-bias pA and pp collisions at the LHC $\sqrt{S} = 8.8$ TeV at different rapidities of the produced hadron η_h and prompt photon η_γ.

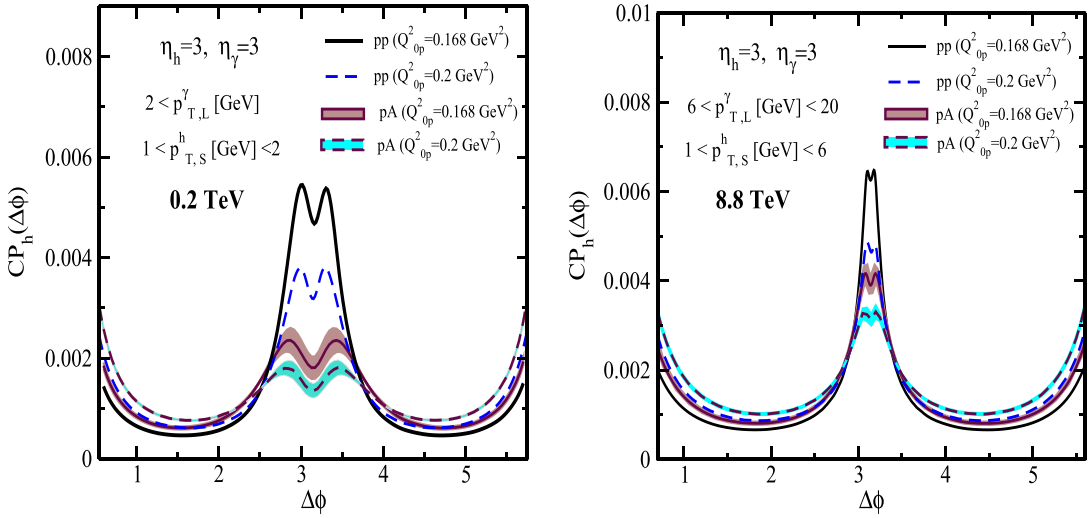

FIG. 7 (color online). The $\gamma - \pi^0$ azimuthal correlation $CP_h(\Delta\phi)$ in minimum-bias pA and pp collisions at forward rapidity at RHIC and the LHC. The curves are obtained by the rcBK equation with two different initial saturation scales of proton $Q_{0p}^2 = 0.168$ and 0.2 GeV^2 and the corresponding initial saturation scale of the nucleus within $Q_{0A}^2 = 3 \div 4Q_{0p}^2$.

to $\gamma = 1.19$ and $\gamma = 1$ in Eq. (13), respectively [19], and the initial saturation scale of nuclei (gold and lead) within $Q_{0A}^2 = 3 \div 4Q_{0p}^2$. Although both values of Q_{0p} (or γ) are extracted from a fit to HERA data on the proton target at small-x [19] (with a good χ^2), the recent LHC data seems to favor the parameter set with $\gamma > 1$ (or lower value for Q_{0p}) [8]. The uncertainties in the initial scale for proton will bring even larger uncertainties in determining the parameters of the rcBK equation for the case of nuclear target.[3] Therefore, the upcoming LHC data on pA collisions can provide a crucial complementary constrain on the rcBK evolution equation and small-x physics. For other measurements sensitive to the saturation physics at the LHC, see Refs. [9,12,32].

Note that the semi-inclusive photon-hadron cross section in Eq. (1) has collinear singularity. Therefore, one should first treat the collinear singularity for the near-side jet $\Delta\phi \approx 0$ in a same fashion as was done for the inclusive prompt photon production in Eq. (4) by introducing the quark-photon fragmentation function. Therefore, our results at near-side $\Delta\phi \approx 0$ should be less reliable. However, one should bear in mind that the integrand in the azimuthal correlation generally samples lower transverse momenta for the away-side correlations $\Delta\phi \approx \pi$ than for near-side ones $\Delta\phi \approx 0$. Therefore, here we only focused on the away-side correlations which is a sensitive probe of small-x physics and gluon saturation.

In Fig. 8, we show the nuclear modification factor $R_{pA}^{h\gamma}$ for semi-inclusive photon-hadron pair production defined in Eq. (17) as a function of $\Delta\phi$ at the LHC energy $\sqrt{S} = 8.8$ TeV and $\eta_h = \eta_\gamma = 3$ for two different transverse momenta bins of produced prompt photon p_T^γ and hadron p_T^h (the integral is performed over the given interval of transverse momenta). Similar to previous plots, the band [CGC-rcBK-average] in Fig. 8 comes from the rcBK solutions incorporating the uncertainties associated to a variation of the initial saturation scale of the nucleus in a range consistent with previous studies of DIS structure functions as well as particle production in minimum-bias pp, pA, and AA collisions in the CGC formalism. One may therefore expect that the possible effects of fluctuations on particle production is effectively contained in our error band. The away-side nuclear modification $R_{pA}^{h\gamma}$ at $\Delta\phi \approx \pi$ is dramatically suppressed with a lower peak structure when the transverse momentum bin of the produced prompt photon is larger than hadron $z_T < 1$. This is fully in accordance with the photon-hadron decorrelation in pA compared to pp collisions, and conditions given in Eqs. (20) and (21) for the existence of the local minimum for the away-side photon-hadron production. Note that the sensitivity to the transverse momenta or the ratio z_T only manifests itself at around $\Delta\phi \approx \pi$.

Finally, in Fig. 9, we show the two-dimensional nuclear modification factor $R_{pA}^{h\gamma}$ for semi-inclusive photon-hadron production defined in Eq. (18) as a function of transverse momentum of produced prompt photon p_T^γ and hadron p_T^h at RHIC $\sqrt{S} = 0.2$ TeV at $\eta_h = \eta_\gamma = 4$ (top panel) and at the LHC $\sqrt{S} = 8.8$ TeV at $\eta_h = \eta_\gamma = 3$ (lower panel). The area between two surfaces in Fig. 9, similar to Fig. 8 (the band labeled by CGC-rcBK-av) shows the uncertainties associated to the variation of the initial saturation scale of the nucleus. It is seen that at the LHC energy $\sqrt{S} = 8.8$ TeV, the nuclear modification factor $R_{pA}^{h\gamma}$ is

[3]This is partly due to the fact that solution of the rcBK equation in the presence of impact parameter is not yet available.

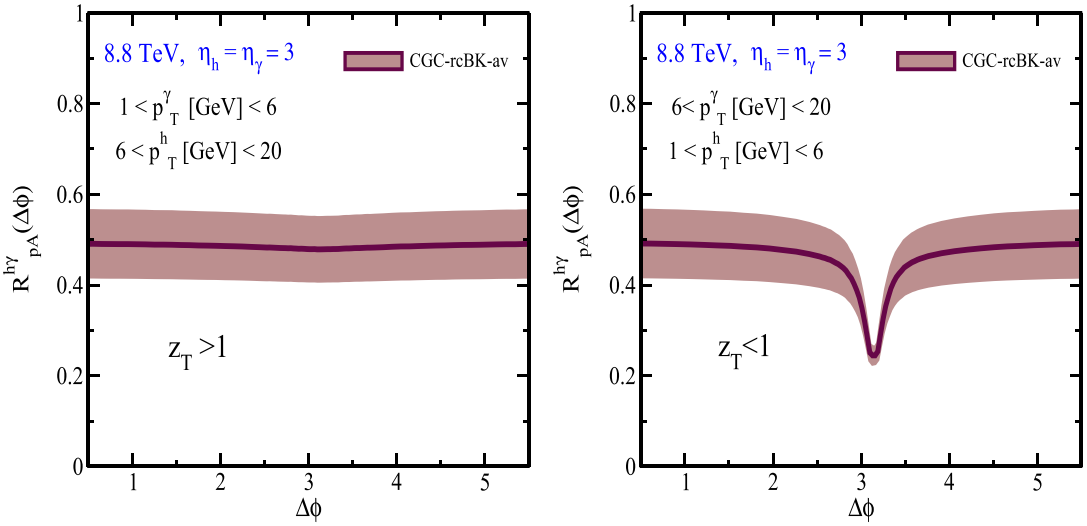

FIG. 8 (color online). The nuclear modification factor $R^{h\gamma}_{pA}$ for semi-inclusive photon-hadron ($\gamma - \pi^0$) production defined in Eq. (17) as a function of $\Delta\phi$ at the LHC in minimum-bias pA collisions at forward rapidity $\eta_h = \eta_\gamma = 3$ for two different bins of transverse momenta of produced prompt photon p^γ_T and hadron p^h_T, namely, $z_T < 1$ (right) and $z_T > 1$ (left). The band (CGC-rcBK-average) incorporates the uncertainties due to variation of the initial saturation scale in the rcBK evolution equation.

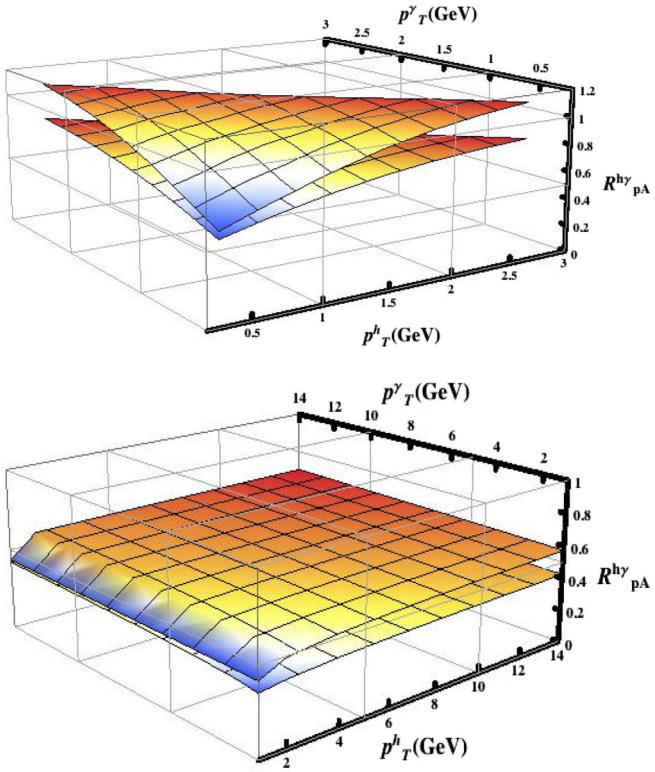

FIG. 9 (color online). The nuclear modification factor $R^{h\gamma}_{pA}$ for semi-inclusive $\gamma - \pi^0$ production defined in Eq. (18) as a function of transverse momentum of produced prompt photon p^γ_T and hadron p^h_T in minimum-bias pA collisions at RHIC $\sqrt{S} = 0.2$ TeV at $\eta_h = \eta_\gamma = 4$ (top panel) and the LHC $\sqrt{S} = 8.8$ TeV at $\eta_h = \eta_\gamma = 3$ (lower panel). Two surfaces are obtained from the solutions of the rcBK evolution equation with two different initial saturation scales of the nucleus; see the text for the details.

more suppressed compared to RHIC and also is more flat. We recall that the semi-inclusive photon-hadron cross section Eq. (1) is not equal to the product of cross sections of single inclusive prompt photon and hadron production given in Eqs. (4) and (7). Note that in Ref. [12] it was shown that at RHIC for the single inclusive prompt photon production, a good portion of the suppression at forward rapidities is due to the projectile being a deuteron rather than a proton. Here for a comparison with pA run at the LHC energy and in order to discard possible suppression associated to isospin effect [12], we have only considered proton-nucleus collisions at the RHIC energy, which can be also useful for the future pA run at RHIC. We check that similar to Ref. [12], discarding the fragmentation photon contribution from the cross section, will not affect our results for $R^{h\gamma}_{pA}$ significantly. Nevertheless, a detailed study of the semi-inclusive photon-hadron production in the presence of isolation cut is beyond the scope of the current paper.

V. SUMMARY

We have investigated semi-inclusive prompt photon-hadron production in high-energy pp and pA collisions within the CGC framework by using the running-coupling BK equation. We provided detailed predictions for the coincidence probability of photon-hadron correlations and showed that such correlations exhibit novel features, namely, that the away-side correlations can have a double- or single-peak structure depending on the trigger particle selection and kinematics. The correlations have a double-peak structure by selecting $\gamma - h$ pairs within the kinematics region satisfying the conditions in

Eqs. (20) and (21), and the away-side double-peak correlations will evolve to a single-peak structure for kinematics outside of that region. We showed that this feature can be understood by QCD saturation dynamics. The double-peak structure for the azimuthal correlations has also been recently reported for other electromagnetic probes, namely, the Drell-Yan Lepton-Pair-Jet correlation in pA collisions [41] while it is absent for dihadron production [13,23]. The decorrelation of the away-side photon-hadron production with energy, rapidity, density, and transverse momentum of the probe is very similar to the dihadron production in pA collisions and can be understood in the CGC framework. If experimentally confirmed, this will provide significant evidence in favor of the universality of particle production in the QCD saturation picture at high energy.

In a sense, the double-peak structure for $\gamma - h$ correlations resembles the long-range azimuthal correlations for the produced charged hadron pairs, observed in high-multiplicity events in pp collisions at the LHC, the so-called ridge phenomenon [42]. Although, the ridge is a feature on a near-side $\Delta\phi \approx 0$ of the two-particle correlations, while the $\gamma - h$ double-peak structure is a away-side feature. In both cases, a second local maximum occurs because of angular collimation due to the presence of the saturation scale in the system, and the effect shows up within a kinematics window which is dictated by the saturation scale[4] [10,11,43]. Similar to the ridge, the double-peak structure here can survive up to rather large rapidity (see Fig. 6), and in both cases, one expects that the same mechanism to be responsible for the self-deconstruction of the effect, namely, decorrelation at very high energy [43].

We also showed that the ratio $z_T = p_T^h/p_T^\gamma$ is a sensitive parameter to the saturation region and controls the away-side $\gamma - h$ suppression in high-energy pp and pA collisions.

We studied the ratio of single inclusive prompt photon to hadron production $\gamma^{\text{inclusive}}/\pi^0$ in pp and pA collisions at RHIC and the LHC at various rapidities. We found that the ratio $\gamma^{\text{inclusive}}/\pi^0$ is very similar for high-energy pp and pA collisions at forward rapidities at high transverse momentum, and it increases with rapidity while it decreases with energy. We also provided predictions for the nuclear modification factor for the semi-inclusive photon-hadron pair production $R_{pA}^{h\gamma}$ in pA collisions at RHIC and the LHC at forward rapidities. We showed that the two-dimensional $R_{pA}^{h\gamma}$ is generally more flat at the LHC compared to the RHIC at forward rapidities. We found that the suppression of the nuclear modification factor for semi-inclusive photon-hadron production is comparable to that for single inclusive hadron [32] and prompt photons [12] production in pA collisions at forward rapidities.

[4]The author thanks Raju Venugopalan for pointing out the possible similarity between these two phenomena.

ACKNOWLEDGMENTS

The author would like to thank Thomas Peitzmann and Richard Seto for useful discussions which led to this paper. The author is grateful to Raju Venugopalan for a careful reading of the manuscript and useful comments. It is a great pleasure to thank Adrian Dumitru and Jamal Jalilian-Marian for fruitful conversations at the early stage of this work. This work is supported in part by Fondecyt Grant No. 1110781.

[1] L. V. Gribov, E. M. Levin, and M. G. Ryskin, Phys. Rep. **100**, 1 (1983); A. H. Mueller and J-W. Qiu, Nucl. Phys. **268**, 427 (1986).
[2] L. D. McLerran and R. Venugopalan, Phys. Rev. D **49**, 2233 (1994); **49**, 3352 (1994); **50**, 2225 (1994).
[3] E. Iancu, A. Leonidov, and L. McLerran, arXiv:hep-ph/0202270; E. Iancu and R. Venugopalan, arXiv:hep-ph/0303204; F. Gelis, E. Iancu, J. Jalilian-Marian, and R. Venugopalan, Annu. Rev. Nucl. Part. Sci. **60**, 463 (2010) and references therein.
[4] V. Khachatryan *et al.* (CMS Collaboration), Phys. Rev. Lett. **105**, 022002 (2010); K. Aamodt *et al.* (ALICE Collaboration), Phys. Rev. Lett. **105**, 252301 (2010); S. Chatrchyan *et al.* (CMS Collaboration), J. High Energy Phys. 08 (2011) 141; G. Aad *et al.* (ATLAS Collaboration), Phys. Lett. B **710**, 363 (2012).
[5] E. Levin and A. H. Rezaeian, Phys. Rev. D **82**, 014022 (2010); **83**, 114001 (2011).
[6] P. Tribedy and R. Venugopalan, Nucl. Phys. **A850**, 136 (2011); Nucl. Phys. **A859**, 185 (2011); A. Dumitru and Y. Nara, Phys. Rev. C **85**, 034907 (2012).
[7] D. Kharzeev, E. Levin, and M. Nardi, Nucl. Phys. **A747**, 609 (2005).
[8] J. L. Albacete and A. Dumitru, arXiv:1011.5161.
[9] A. H. Rezaeian, Phys. Rev. D **85**, 014028 (2012); arXiv:1208.0026; arXiv:1110.6642; E. Levin and A. H. Rezaeian, Phys. Rev. D **82**, 054003 (2010); AIP Conf. Proc. **1350**, 243 (2011).
[10] A. Dumitru, K. Dusling, F. Gelis, J. Jalilian-Marian, T. Lappi, and R. Venugopalan, Phys. Lett. B **697**, 21 (2011); K. Dusling and R. Venugopalan, Phys. Rev. Lett. **108**, 262001 (2012).
[11] E. Levin and A. H. Rezaeian, Phys. Rev. D **84**, 034031 (2011).
[12] J. Jalilian-Marian and A. H. Rezaeian, Phys. Rev. D **86**, 034016 (2012).

[13] C. Marquet, Nucl. Phys. **A796**, 41 (2007); K. Tuchin, Nucl. Phys. **A846**, 83 (2010); J. L. Albacete and C. Marquet, Phys. Rev. Lett. **105**, 162301 (2010); F. Dominguez, B. W. Xiao, and F. Yuan, Phys. Rev. Lett. **106**, 022301 (2011); F. Dominguez, C. Marquet, B.-W. Xiao, and F. Yuan, Phys. Rev. D **83**, 105005 (2011); A. Stasto, B.-W. Xiao, and F. Yuan, Phys. Lett. B **716**, 430 (2012); K. Kutak and S. Sapeta, arXiv:1205.5035; T. Lappi and H. Mäntysaari, arXiv:1207.6920.

[14] F. Gelis and J. Jalilian-Marian, Phys. Rev. D **66**, 014021 (2002); R. Baier, A. H. Mueller, and D. Schiff, Nucl. Phys. **A741**, 358 (2004).

[15] I. Balitsky, Nucl. Phys. **B463**, 99 (1996); Y. V. Kovchegov, Phys. Rev. D **60**, 034008 (1999); Phys. Rev. D **61**, 074018 (2000).

[16] I. I. Balitsky, Phys. Rev. D **75**, 014001 (2007).

[17] I. Balitsky and G. A. Chirilli, Phys. Rev. D **77**, 014019 (2008); E. Gardi, J. Kuokkanen, K. Rummukainen, and H. Weigert, Nucl. Phys. **A784**, 282 (2007); Y. V. Kovchegov and H. Weigert, Nucl. Phys. **A784**, 188 (2007); E. Avsar, A. M. Stasto, D. N. Triantafyllopoulos, and D. Zaslavsky, J. High Energy Phys. 10 (2011) 138.

[18] J. L. Albacete and Y. V. Kovchegov, Phys. Rev. D **75**, 125021 (2007).

[19] J. L. Albacete, N. Armesto, J. G. Milhano, P. Quiroga Arias, and C. A. Salgado, Eur. Phys. J. C **71**, 1705 (2011).

[20] B. Z. Kopeliovich and A. H. Rezaeian, Int. J. Mod. Phys. E **18**, 1629 (2009).

[21] K. Golec-Biernat and M. Wusthoff, Phys. Rev. D **59**, 014017 (1998); H. Kowalski and D. Teaney, Phys. Rev. D **68**, 114005 (2003); E. Iancu, K. Itakura, and S. Munier, Phys. Lett. B **590**, 199 (2004); H. Kowalski, L. Motyka, and G. Watt, Phys. Rev. D **74**, 074016 (2006); G. Watt and H. Kowalski, Phys. Rev. D **78**, 014016 (2008); E. Gotsman, E. Levin, M. Lublinsky, and U. Maor, Eur. Phys. J. C **27**, 411 (2003); M. Lublinsky, Eur. Phys. J. C **21**, 513 (2001); A. H. Mueller and D. N. Triantafyllopoulos, Nucl. Phys. **B640**, 331 (2002); D. N. Triantafyllopoulos, Nucl. Phys. **B648**, 293 (2003); C. Marquet and G. Soyez, Nucl. Phys. **A760**, 208 (2005).

[22] For example: V. Khachatryan *et al.* (CMS Collaboration), Phys. Rev. Lett. **106**, 122003 (2011); J. High Energy Phys. 09 (2010) 091; J. Adams *et al.* (STAR Collaboration), Phys. Rev. Lett. **91**, 072304 (2003); G. Aad *et al.* (ATLAS Collaboration), Phys. Rev. Lett. **105**, 252303 (2010); S. Chatrchyan *et al.* (CMS Collaboration), Phys. Rev. C **84**, 024906 (2011); K. Aamodt *et al.* (ALICE Collaboration), Phys. Rev. Lett. **108**, 092301 (2012).

[23] A. Adare *et al.* (PHENIX Collaboration), Phys. Rev. Lett. **107**, 172301 (2011); E. Braidot (STAR Collaboration), Nucl. Phys. **A854**, 168 (2011); E. Braidot, Ph.D. thesis, arXiv:1102.0931.

[24] A. Adare *et al.* (PHENIX Collaboration), Phys. Rev. C **80**, 024908 (2009).

[25] X.-N. Wang and Z. Huang, Phys. Rev. C **55**, 3047 (1997); X.-N. Wang, Z. Huang, and I. Sarcevic, Phys. Rev. Lett. **77**, 231 (1996); H. Zhang, J. F. Owens, E. Wang, and X.-N. Wang, Phys. Rev. Lett. **103**, 032302 (2009); G.-Y. Qin, J. Ruppert, C. Gale, S. Jeon, and G. D. Moore, Phys. Rev. C **80**, 054909 (2009).

[26] J. Jalilian-Marian, A. Kovner, A. Leonidov, and H. Weigert, Nucl. Phys. **B504**, 415 (1997); Phys. Rev. D **59**, 014014 (1998); E. Iancu, A. Leonidov, and L. D. McLerran, Nucl. Phys. **A692**, 583 (2001); E. Ferreiro, E. Iancu, A. Leonidov, and L. D. McLerran, Nucl. Phys. **A703**, 489 (2002).

[27] A. Dumitru, J. Jalilian-Marian, T. Lappi, B. Schenke, and R. Venugopalan, Phys. Lett. B **706**, 219 (2011); T. Lappi, Phys. Lett. B **703**, 325 (2011).

[28] J. F. Owens, Rev. Mod. Phys. **59**, 465 (1987).

[29] A. H. Rezaeian and A. Schaefer, Phys. Rev. D **81**, 114032 (2010); B. Z. Kopeliovich, A. H. Rezaeian, H. J. Pirner, and I. Schmidt, Phys. Lett. B **653**, 210 (2007); B. Z. Kopeliovich, E. Levin, A. H. Rezaeian, and I. Schmidt, Phys. Lett. B **675**, 190 (2009); B. Z. Kopeliovich, H. J. Pirner, A. H. Rezaeian, and I. Schmidt, Phys. Rev. D **77**, 034011 (2008); M. V. T. Machado and C. B. Mariotto, Eur. Phys. J. C **61**, 871 (2009).

[30] A. Dumitru, A. Hayashigaki, and J. Jalilian-Marian, Nucl. Phys. **A765**, 464 (2006).

[31] T. Altinoluk and A. Kovner, Phys. Rev. D **83**, 105004 (2011).

[32] J. Jalilian-Marian and A. H. Rezaeian, Phys. Rev. D **85**, 014017 (2012).

[33] J. L. Albacete and C. Marquet, Phys. Lett. B **687**, 174 (2010).

[34] K. Dusling, F. Gelis, T. Lappi, and R. Venugopalan, Nucl. Phys. **A836**, 159 (2010).

[35] K. Golec-Biernat and A. M. Stasto, Nucl. Phys. **B668**, 345 (2003); J. Berger and A. M. Stasto, Phys. Rev. D **84**, 094022 (2011).

[36] N. Armesto, C. A. Salgado, and U. A. Wiedemann, Phys. Rev. Lett. **94**, 022002 (2005).

[37] D. d'Enterria, arXiv:nucl-ex/0302016.

[38] A. D. Martin, W. J. Stirling, R. S. Thorne, and G. Watt, Phys. Lett. B **652**, 292 (2007); A. D. Martin, W. J. Stirling, R. S. Thorne, and G. Watt, Eur. Phys. J. C **63**, 189 (2009).

[39] B. A. Kniehl, G. Kramer, and B. Potter, Nucl. Phys. **B582**, 514 (2000).

[40] L. Bourhis, M. Fontannaz, and J. P. Guillet, Eur. Phys. J. C **2**, 529 (1998); M. Gluck, E. Reya, and A. Vogt, Phys. Rev. D **48**, 116 (1993); Phys. Rev. D **51**, 1427 (1995).

[41] A. Stasto, B-W Xiao, and D. Zaslavsky, Phys. Rev. D **86**, 014009 (2012).

[42] V. Khachatryan *et al.* (CMS Collaboration), J. High Energy Phys. 09 (2010) 091.

[43] A. Kovner and M. Lublinsky, Phys. Rev. D **83**, 034017 (2011); Phys. Rev. D **84**, 094011 (2011).